Impact of phenomenological theory of turbulence on pragmatic approach to fluvial hydraulics

Sk Zeeshan Ali, and Subhasish Dey

Impact of phenomenological theory of turbulence on pragmatic approach to fluvial hydraulics

Sk Zeeshan Ali[1,a)] and Subhasish Dey[1,2,3,b)]

[1]*Department of Civil Engineering, Indian Institute of Technology Kharagpur, West Bengal 721302, India*
[2]*Physics and Applied Mathematics Unit, Indian Statistical Institute Kolkata, West Bengal 700108, India*
[3]*Department of Hydraulic Engineering, State Key Laboratory of Hydro-Science and Engineering,
Tsinghua University, Beijing 100084, China*

The phenomenological theory of turbulence (PTT) remains a long-standing and fascinating theory in turbulence research. In this review article, we highlight the state-of-the-science of the impact of the PTT on the pragmatic approach to fluvial hydraulics, explored over recent decades, discussing the salient and the subtle roles that the turbulence plays in governing many physical processes. To acquire a theoretical explanation of this pragmatic approach necessitates an intuitive thought that can bring together the background mechanisms of all the physical processes under one law—a thought that is capable of finding their inextricable links with the turbulent energy spectrum. We begin here with emphasizing the spectral and the co-spectral origin of the well-recognized laws of the wall, the resistance equation, and the turbulence intensities by portraying the typical momentum transfer mechanism of eddies in a turbulent flow. Next, we focus on the scaling laws of key fluvial processes derived from the perspective of the PTT, enlightening their physical insight and ability to judge how far the so-called empirical formulas can be used with confidence. The PTT has been able to disclose the origin of several primeval empirical formulas that have been used over many years without having any theoretical clarification and confirmation. Finally, we make an effort to describe some unsolved issues to be resolved as a future scope of research. *Published by AIP Publishing.*
https://doi.org/10.1063/1.5025218

I. INTRODUCTION

Nobel Laureate Werner Heisenberg, on his death-bed, was reported to have uttered, "When I meet God, I am going to ask him two questions: Why relativity? And why turbulence? I really believe he will have an answer for the first." This statement makes it clear that our knowledge of turbulence remains rather incomplete. Turbulence oversees a lot of physical phenomena on our planet and beyond. It manifests a wide range of scales in which the large-scales, commensurate with the scale of the physical domain, possess most of the turbulent kinetic energy, whereas their descendant small-scales dissipate most of the turbulent kinetic energy by fluid viscosity. A central trait in the understanding of turbulence is the existence of Richardson's cascades of excitations, which evolve in five dimensions,[1] from large to small scales or vice versa. A persistent concept in the phenomenology of turbulence is the small-scale universality, evidenced by the groundbreaking theories, laboratory measurements, and numerical simulations.[2–8] Despite a milestone of turbulence theories, predictive model for a wall-shear flow remains a challenging task due to several complexities.[9]

In fluvial hydraulics, turbulent flow plays a subtle role to govern a variety of natural phenomena, which have a profound, although subtle, impact on geomorphology, engineering, climate dynamics, and many others. These phenomena evolve in space and time, involving several scaling laws that are important from the perspective of education, research, and practice. Many primitive empirical formulas, available in standard textbooks of fluvial hydraulics, authenticated by extensive laboratory and field measurements appear to have served many purposes over several decades. In fact, the pragmatic approach to fluvial hydraulics dates back to the celebrated resistance formulas, as given in the book by Dey.[10] Although these formulas overlie the empirical foundation, they have been used over many years without searching for a sagacious explanation from the perspective of the *phenomenological theory of turbulence* (PTT). Rapid advances made in the turbulence research, especially in recent decades, have unraveled this important aspect. One of the outstanding achievements was to find the missing link between the shear stress and the turbulent energy spectrum.[11] This link has explained many unsolved problems, for instance, the origin of the well-recognized laws in a wall-shear flow.

The application of the PTT in recent years has become a rule of thumb to seek the origin of the scaling laws involved in various physical processes in a fluvial system, particularly when the sediment particles accompany the turbulent flow. The scaling laws provide an insight into the physical phenomena, where the turbulence leaves its profound signature. Such scaling laws derived from the perspective of the PTT provide a genuine ground to check the veracity of the empirical

a)Author to whom correspondence should be addressed: skzeeshanali@
iitkgp.ac.in
b)sdey@iitkgp.ac.in

formulas and can build a promising synergy between the theory and the practice. The derivation steps encompass the fundamental tenets of turbulence laws, the similarity hypotheses, and the phenomenological arguments.[2,3] However, it is pertinent to mention that the PTT can effectively predict the scaling laws in terms of the mathematical expression for a physical phenomenon involving turbulence, but it cannot predict the proportionality constant. In this review article, we exemplify the state-of-the-science of the impact of the PTT by highlighting its elegance and straightforwardness on the pragmatic approach to fluvial hydraulics; however, we showcase its widespread significance by briefly referring to other physical phenomena in nature.

II. WALL-SHEAR FLOW

In a wall-shear flow, we shed light on the origin of the *law of the wall*, the *resistance equation*, and the *turbulence intensities* from the perspective of the PTT. We focus on the link between the friction factor and the turbulent energy spectrum by referring to two elegant theories developed in recent years, labeled as the *spectral theory*[12] and the *co-spectral budget theory*.[13] These theories primarily apply to obtain the fluid shear stress at a finite distance from a reference level due to the momentum transfer caused by the turbulent eddies, relating the fluctuations of the eddies with the unique properties of the turbulent energy spectrum. The underlying mechanisms in seeking the scaling laws of the law of the wall, the resistance equation, and the turbulence intensities with certain plausible assumptions are appraised below.

A. The law of the wall

The classical law of the wall describes the law of velocity slowdown within the turbulent wall-shear layer and it acts as a benchmark for predicting the skin-frictional drag in a pipeline or an aircraft. It is also recognized as a fundamental law in fluvial hydraulics and geomorphology to determine the shear stress exerted at the surface of a granular bed.[10] This law states that the time-averaged flow velocity $\bar{u}$ within the turbulent wall-shear layer obeys a logarithmic scaling law with the vertical distance z measured from the channel bed. It is expressed as

$$\bar{u}(z) = \frac{u_*}{\kappa} \ln \frac{z}{z_0}, \tag{1}$$

where $u_* [= (\tau_0/\rho_f)^{1/2} = (ghS_0)^{1/2}]$ is the shear velocity, τ_0 is the bed shear stress, ρ_f is the mass density of fluid, g is the gravitational acceleration, h is the flow depth, $S_0 (= \tan^{-1} \chi)$ is the streamwise slope of the channel bed, χ is the streamwise

inclination of the channel bed, κ (= 0.41) is the von Kármán constant, and z_0 is the zero-velocity level. The law of the wall together with Kolmogorov's theory[2] belongs to the most stirring phenomenological theories of turbulence and is deemed to have received considerable awareness with multifarious interpretations.[14,15] The link between the law of the wall and the Kolmogorov scaling laws was discovered with the aid of the incomplete similarity, the intermediate asymptotics, and the composite expansions, which were discussed elsewhere,[15–17] and also appraised via the spectral theory[12,18,19] and the co-spectral budget theory.[13,20] In this context, it is worth emphasizing that the law of the wall was obtained from the assumption of a constant stress flow layer, called the wall-shear layer. This assumption of constant stress is debatable.[14]

The spectral theory reveals that the time-averaged velocity distribution in a boundary layer flow is connected with the shape of the turbulent energy spectrum.[12] To gain an insight into the law of the wall from the perspective of the PTT, let us first consider the schematic representation of the physical system as illustrated in Fig. 1, where an open-channel flow, being turbulent, has a flow depth h and a mean flow velocity U. The enlarged frame of the channel bed depicts the bed roughness of uniform size r in succession.

Figure 2 shows the detail derivation of the law of the wall involved in the spectral theory. In accordance with the spectral theory, the Reynolds shear stress τ developed at a surface $S(z)$ due to a turbulent eddy of size l, having a characteristic velocity v_l, is the product of the velocity difference resulting in a momentum contrast across the eddy and the eddy turnover velocity. It follows

$$\tau = -\rho_f \overline{u'w'} \sim \rho_f \Gamma l v_l = \rho_f \kappa_\tau \Gamma l v_l, \tag{2}$$

where u' and w' are the velocity fluctuations in horizontal and vertical directions, respectively, the overline refers to the time-averaging, $\Gamma (= d\bar{u}/dz)$ is the local strain rate, and κ_τ is a coefficient. The v_l was determined from the integration of the turbulent energy spectrum over the eddy wavenumber k ranging from l^{-1} to ∞. In identifying the prevailing turbulent eddies straddling the surface $S(z)$, it was argued that the eddies of size larger than z contribute feebly to the net momentum transfer because these eddies are unable to straddle the $S(z)$ completely. It implies that the prevailing eddies straddling the $S(z)$ are the eddies of size $l = z$ (or $kz = 1$) yielding $v_z = (\kappa_\varepsilon \varepsilon z)^{1/3}$, where κ_ε is a coefficient and ε is the turbulent kinetic energy dissipation rate. Within the turbulent wall-shear layer, applying the energy balance equation, $\rho_f \varepsilon = \Gamma \tau = \rho_f \Gamma u_*^2$ produces the local strain rate

$$\Gamma = \frac{u_*}{(\kappa_\tau^3 \kappa_\varepsilon)^{1/4} z}, \tag{3}$$
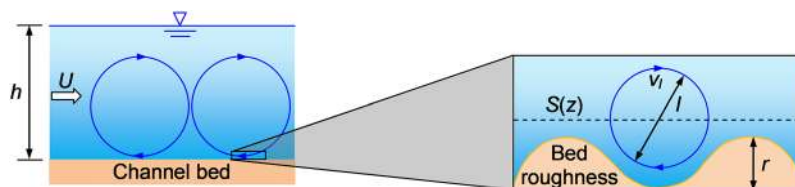
FIG. 1. Schematic illustration of flow through a turbulent channel (*left*), having a flow depth h and a mean flow velocity U. The enlarged frame of the channel bed (*right*) illustrates the typical momentum transfer mechanism at a surface $S(z)$, parallel to the line touching the summit of the bed roughness, due to a local turbulent eddy of size l, having a characteristic velocity v_l, in the proximity of the channel bed characterized by the bed roughness of size r.
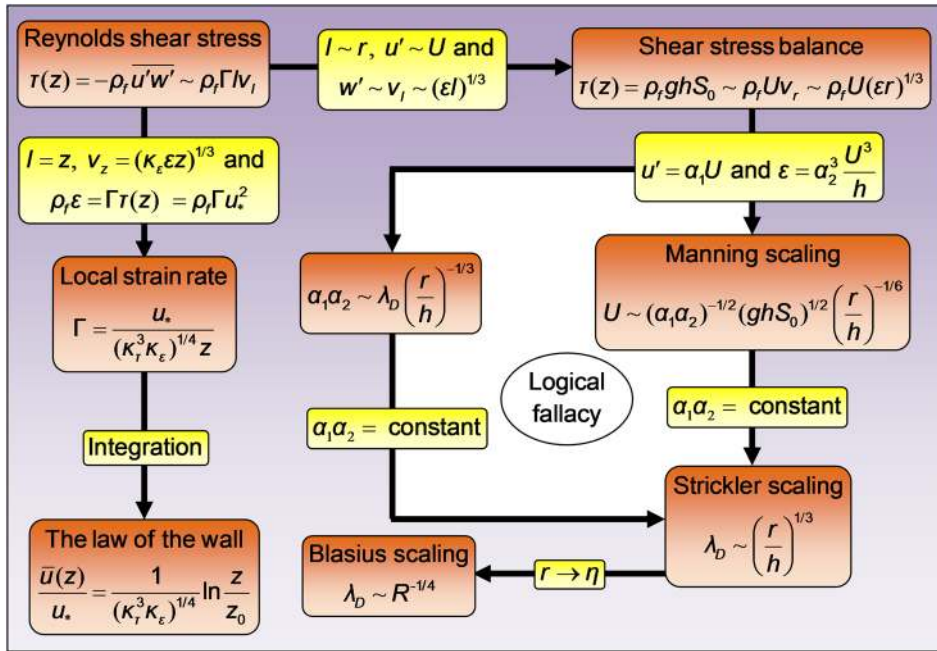
FIG. 2. Schematic illustration of the derivations of the law of the wall and the resistance equation by means of the spectral theory.[12,18,19]

which can be integrated to obtain the law of the wall [Eq. (1)], having the von Kármán constant $\kappa = (\kappa_\tau^3 \kappa_\varepsilon)^{1/4}$. Since eddies in the wall-shear layer belong to the equilibrium range (that is, the energy inertial range), the Kolmogorov four-fifth law can be readily applied. Thus, using $\kappa_\varepsilon = 4/5$ and $\kappa = 0.41$ results in $\kappa_\tau = 0.33$.

The co-spectral budget theory presents a comprehensive scrutiny of the spectral theory and unfolds the weakness of the spectral theory on many facets, for instance, in the spectral theory, the v_l can be solely linked with the turbulent energy spectrum rather than the vertical velocity spectrum. Moreover, the spectral theory disregards the contributions from the enstropy term in the momentum balance. Thus, the co-spectral budget theory offers new insights into the momentum transfer mechanism by providing an improvement of the lacunas of the spectral theory. Figure 3 shows the generalized co-spectral budget, where $F_{wu}(k)$ is the co-spectrum function, t is the time, ν is the coefficient of kinematic viscosity of fluid, $P_{wu}(k)$ $[= \Gamma E_{ww}(k)]$ is the production term, E_{ww} is the energy spectrum function of the vertical velocity, $T_{wu}(k)$ is the co-spectral flux transport term, and $\Pi(k)$ is the velocity-pressure correlation term. After certain approximations, the solution for the $F_{wu}(k)$ was obtained as

$$F_{wu}(k) = A^{-1} \Gamma \varepsilon^{-1/3} E_{ww}(k) k^{-2/3}, \tag{4}$$
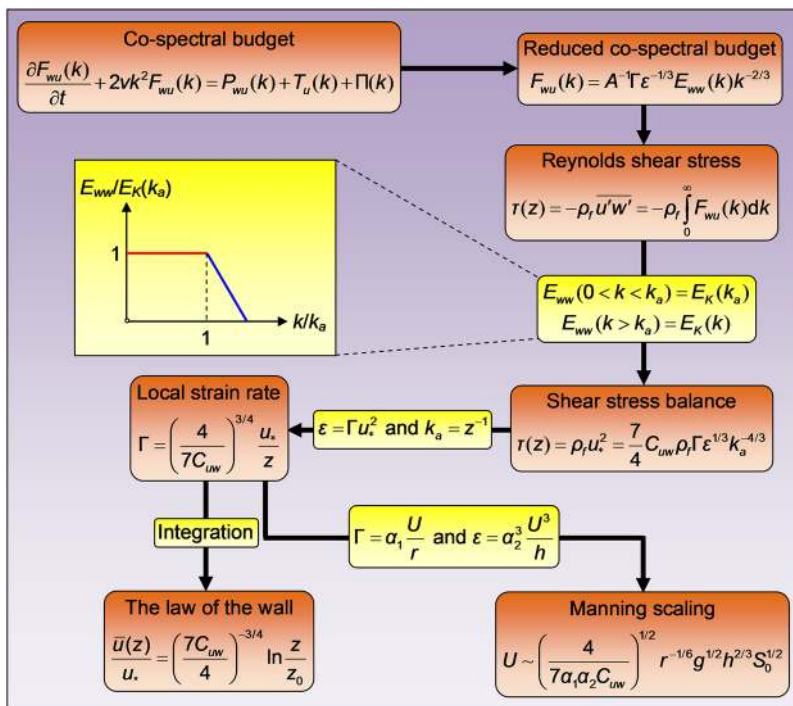
FIG. 3. Schematic illustration of the derivations of the law of the wall and the resistance equation by means of the co-spectral budget theory.[13,20]

where $A = C_R/(1 - C_I)$, C_R $(= 1.8)$ is the Rotta constant and $C_I = 3/5$, in agreement with the rapid distortion theory of isotropic turbulence.[13,20] Fundamentally, the C_I is linked with the isotropization of the production term that corrects the original model proposed by Rotta (see Ref. [13]). The Reynolds shear stress $\tau(z)$ can be obtained by integrating the co-spectrum function $F_{wu}(k)$ encompassing the full range of the eddy wavenumber k (Fig. [3]). To evaluate this integral, it was necessary to express the $E_{ww}(k)$ as a function of k. To this end, the $E_{ww}(k)$ was linked with the Kolmogorov spectrum function E_K as $E_{ww}(k \leq k_a) = E_K(k_a)$ and $E_{ww}(k > k_a) = E_K(k)$ (Fig. [3]). This idealized scenario of the spectrum function delineates the sudden switchover of the $E_{ww}(k)$ from a constant value to the universal wavenumber dependency in the energy inertial range. This consideration overlooked the low wavenumber modulations $kh \to 1$ and the Pao correction $k\eta \to 1$, where η $[= (v^3/\varepsilon)^{1/4}]$ is the Kolmogorov length scale.[21] This spectral depiction was supported by ample laboratory and field experimental data.[21] Moreover, the breakpoint at $k = k_a$ respects Townsend's attached eddy hypothesis.[22] The $E_K(k)$ can be expressed in the phenomenological form as $E_K(z^{-1} \ll k \ll \eta^{-1}) = C_0 \varepsilon^{2/3} k^{-5/3}$, where $C_0 = (24/55)C_K$ and C_K $(= 1.5)$ is the Kolmogorov constant for three-dimensional (3D) wavenumbers. It is pertinent to note that when $E_{ww}(k) = E_K(k)$, $F_{wu}(k) = C_{uw}\Gamma\varepsilon^{1/3}k^{-7/3}$, corroborating the other co-spectral theories and the experimental measurements.[23,24] Here, C_{uw} $(= A^{-1}C_0)$ is a coefficient with a constant value of 0.15. With this form of $E_{ww}(k)$ and following the stress balance $(-\rho_f \overline{u'w'} = \rho_f u_*^2)$, the energy balance $(\rho_f \varepsilon = \rho_f \Gamma u_*^2)$, and noting $k_a = z^{-1}$, the local strain rate reads

$$\Gamma = \left(\frac{4}{7C_{uw}}\right)^{3/4} \frac{u_*}{z}, \quad (5)$$

which upon integration produces the law of the wall [Eq. [(1)]], with the von Kármán constant $\kappa = (7C_{uw}/4)^{3/4} = 0.37$. This shows that the co-spectral budget theory provides an underestimation of the von Kármán constant $(= 0.41)$.

Furthermore, the co-spectral budget theory provides an understanding on the suitability of using the law of the wall or the *power law*, which acts as a surrogate for the law of the wall, to define the velocity distribution within the turbulent wall-shear layer. In fact, both the velocity laws can be deduced depending on the proper formulation of the intermittency correction applied to the $E_{ww}(k)$.[13] The intermittency correction modifies the spectrum function as $E_{ww}(k) = C_0 \varepsilon^{2/3} k^{-5/3}(kL)^{\gamma}$, where L is the length scale of large-scale eddies, γ $(= -\mu/9)$ is the intermittency correction, and μ is the intermittency exponent. When $L = z$, the $E_{ww}(kz > 1) = C_0 \varepsilon^{2/3} k^{-5/3}(kz)^{\gamma}$, whereas for $kz \leq 1$, the scaling in the energy inertial range does not exist. With this form of $E_{ww}(k)$, the application of the energy equation and the co-spectral budget preserves the law of the wall; however, it creates a weak dependency of the von Kármán constant on the intermittency exponent. On the other hand, when $L = h$, the co-spectral budget recovers the power law.[13]

B. Resistance equation

The most familiar resistance equation in fluvial hydraulics is the *Manning equation*, which is rigorously used by the researchers belonging to the planetary community. The Manning equation was honored with the title "one of the best formulas of the day."[25] It was also applied to calculate the massive flow in the Martian channels.[26] The Manning equation, proposed in 1891, describes the mean flow velocity U of a fully developed steady-uniform turbulent channel. For a wide rectangular channel, it takes the form[10]

$$U = \frac{1}{n} h^{2/3} S_0^{1/2}, \quad (6)$$

where n is the Manning roughness coefficient in SI units. In essence, for a channel of arbitrary cross section, the h appearing in Eq. [(6)] is to be replaced by the channel hydraulic radius, which is expressed as a ratio of the channel cross-sectional area to the channel wetted perimeter.[10] Although the Manning equation is solely founded on the empirical ground supporting a large corpus of the experimental data, no equation till date is deemed to have replaced the Manning equation. However, the Manning equation in conjunction with the *Strickler scaling* awaited a hundred and eleven years to receive a theoretical explanation, which was given after the advent of the spectral theory that used the incomplete similarity principle.[11]

Reverting to Fig. [1], we note that at the horizontal surface touching the summit of the bed roughness, the local eddies that fill the roughness trough are of size $l \sim r$, and thereby, the local strain rate at this level can be approximated as $\Gamma \sim U/r$ yielding $u' \sim U$ (Fig. [2]). This simplification associated with $v_r \sim (\varepsilon r)^{1/3}$ makes

$$\tau = -\rho_f \overline{u'w'} \sim \rho_f U(\varepsilon r)^{1/3}. \quad (7)$$

The relationship $u' \sim U$ can be further expressed as $u' = \alpha_1 U$ (Fig. [2]), where α_1 is a coefficient.[11,27] In addition, at the summit of the bed roughness, the ε in appearing in Eq. [(7)] can be scaled as $\varepsilon = \alpha_2^3 U^3/h$, where α_2 is a coefficient.[11] Therefore, after the stress balance $(\tau = \tau_0 = \rho_f g h S_0)$, Eq. [(7)] produces the Manning scaling as (also see Fig. [2])

$$U \sim (\alpha_1 \alpha_2)^{-1/2}(ghS_0)^{1/2}\left(\frac{r}{h}\right)^{-1/6}. \quad (8)$$

However, the Strickler scaling can only be retrieved from the Manning scaling if the product $\alpha_1 \alpha_2$ remains a constant. Since $\Gamma = \alpha_1 U/r \sim u_*/r$, it turns out that $\alpha_1 \sim \lambda_D^{1/2}$, where λ_D is the Darcy-Weisbach friction factor $(\sim u_*^2/U^2)$. Moreover, at $z = r$, the ε can be expressed as $\varepsilon = -\overline{u'w'}\Gamma \sim u_*^3/r$. This relationship together with $\varepsilon = \alpha_2^3 U^3/h$ produces $\alpha_2 \sim \lambda_D^{1/2}(r/h)^{-1/3}$. Therefore, a close inspection of the phenomenological arguments prior to derive the Manning scaling unveils that $\alpha_1 \alpha_2 \sim \lambda_D(r/h)^{-1/3}$, which would attain a constant value inasmuch as the λ_D obeys the Strickler scaling, that is, $\lambda_D \sim (r/h)^{1/3}$. This observation reveals a *logical fallacy* of the spectral theory that has been identified recently (Fig. [2] and Ref. [28]).

To get rid of the fallacy, the co-spectral budget theory was applied to derive the Manning scaling independently without inviting the Strickler scaling (Fig. [3]). At the summit of the bed roughness, using the previous phenomenological arguments $(\Gamma = \alpha_1 U/r$ and $\varepsilon = \alpha_2^3 U^3/h)$ and noting $k_a \sim r^{-1}$, the local strain rate Γ gives rise to the Manning scaling as

$$U \sim \left(\frac{4}{7\alpha_1 \alpha_2 C_{uw}}\right)^{1/2} r^{-1/6} g^{1/2} h^{2/3} S_0^{1/2}, \quad (9)$$

where the Manning roughness coefficient n is scaled as $n \sim [4/(7\alpha_1\alpha_2 C_{uw})]^{-1/2}$.[28] Nevertheless, the co-spectral budget theory remains so far silent to provide a theoretical explanation of the Strickler scaling from the perspective of the general properties of the turbulent energy spectrum.

With regard to the spectral theory, it is worth emphasizing that when the bed roughness r approaches the Kolmogorov length scale η resulting in a hydraulically smooth flow, the momentum transfer becomes viscous. Recalling $\eta = (\nu^3/\varepsilon)^{1/4}$ and setting $\eta/h \sim R^{-3/4}$, where R ($= 4Uh/\nu$) is the Reynolds number, the Strickler scaling produces the well-recognized *Blasius scaling* $\lambda_D \sim R^{-1/4}$ (Fig. 2).

It is relevant to discuss here that in case of flow over a rough-permeable channel bed, for instance, a gravel bed, a vegetated, or a snow-covered bed, the resistance to flow departs from its conventional behavior. To address this anomaly, a conceptual framework was developed by extending the spectral theory to flow in a rough-permeable bed.[29] This framework considered the turbulent momentum exchange between the interstitial and the superficial flows via the canonical scales of turbulent eddies.

C. Turbulence intensities

Turbulence intensities play a decisive role in many engineering and industrial applications, for instance, the design of aerodynamic bodies to control the aerofoil drag affecting the fuel efficiency and aerofoil stability,[30] the manoeuvre of Formula One racing cars that produce large turbulent clouds,[31] the generation of premeditated turbulent mixing in industrial flows,[32] and many others. In the realm of fluvial hydraulics, knowledge of turbulence intensities is a prerequisite for the design and operation of hydraulic structures. We first describe the vertical turbulence intensity σ_w, which was derived from the shape of the vertical velocity spectrum $E_{ww}(k)$ as displayed in Fig. 3. Integrating the $E_{ww}(k)$ over limits $k = 0$ to ∞ and using the energy balance equation ($\rho_f \varepsilon = \rho_f \Gamma u_*^2$) together with $k_a = z^{-1}$ produce

$$\sigma_w \approx 1.7 u_*, \tag{10}$$

which is independent of z.[13] This estimation of σ_w was slightly larger than the traditional values (ranging from 1.25 to 1.30) for the boundary layer flows.[10,21] However, the low wavenumber modulations and the exponential cutoff could reduce the predicted value of σ_w. On the other hand, the origin of the logarithmic scaling of the horizontal turbulence intensity σ_u was probed by applying the co-spectral budget theory;[33] and later, a more generalized logarithmic scaling of the σ_u was explained by the random sweeping decorrelation hypothesis.[34] The σ_u was expressed as[33]

$$\frac{\sigma_u^2}{u_*^2} = B_1 - A_1 \ln\left(\frac{z}{h}\right), \tag{11}$$

where B_1 and A_1 are the coefficients. Based on the experimental measurements, numerical simulations, and analytical models,[35–39] the horizontal velocity spectrum in three separate windows of wavenumber can be expressed as $E_{uu}(0 < k < h^{-1}) = C_1 u_*^2 h$, $E_{uu}(h^{-1} < k < z^{-1}) = C_1 u_*^2 k^{-1}$, and $E_{uu}(z^{-1} < k < \eta^{-1}) = C_{uu}\varepsilon^{2/3}k^{-5/3}$,[33,34] where $C_{uu} = (18/55)C_K$. At $k = z^{-1}$, the continuity restraints on $E_{uu}(k)$ suggest $C_1 = C_{uu}\kappa^{-2/3}$. Then, integrating the $E_{uu}(k)$ over limits

$k = 0$ to η^{-1} by accounting for the three distinct spectral regimes, it yields $A_1 = C_1 = C_{uu}\kappa^{-2/3}$ and $B_1/A_1 = 2.5 - 1.5(\eta/z)^{2/3}$. To get rid of the Reynolds number dependency ($z \gg \eta$), it follows $B_1 = 2.5A_1$.

III. FLUVIAL PROCESSES

In geomorphology and physical geography, the fluvial processes result from a direct interplay between the fluvial channel and the sediment grains, and they refer to the complete sequential processes of formation and development of a fluvial system. Despite their ubiquity on the Earth's surface, their existence was evidenced on other terrestrial surfaces including Mercury, Venus, and Mars.[40,41] Large channels carry a colossal amount of sediments, for instance, the Mississippi River in the United States annually sequesters 406×10^6 tons of sediment to the sea.[42] Sometimes, large channels are named by the color of the sediments that they carry, such as the Big Muddy River, the Yellow River, etc. Many fluvial processes are linked with the energetics of the turbulent flow that plays a subtle role to govern the planetary morphodynamics. Here, we illustrate the unique scaling laws of some of the delicate fluvial processes that have been explored in recent decades.

A. Onset of grain motion

The onset of grain motion is among the striking manifestations of turbulent flow over a granular bed. This phenomenon specifies a critical flow velocity beyond which the grains entrain into the flow (Fig. 4). A necessary condition for this phenomenon to occur is the near-bed flow velocity u or the mean flow velocity U to attain their respective critical values. The concept of near-bed flow velocity invites a considerable degree of uncertainty owing to several intricacies entangled in the local velocity measurements. By contrast, proceeding with the idea of mean flow velocity, we find a more lucid characterization of the critical velocity because the mean flow velocity can be readily obtained from the continuity equation. It is therefore no surprise that in many primitive experiments and analytical modeling, the mean flow velocity rather than the
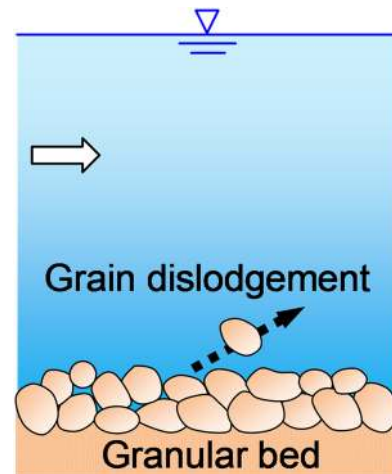
FIG. 4. Schematic illustration of the onset of grain motion.

near-bed flow velocity was considered to be the characteristic critical velocity. In the previous empirical formulas, the nondimensional critical velocity F_{dc} was expressed as a function of relative roughness N (ratio of grain size d to flow depth h) in the following form: $F_{dc} = K f(N)$,[10] where $F_{dc} = U_c/(\Delta g d)^{1/2}$, Δ [$= (\rho_g - \rho_f)/\rho_f$] is the submerged relative density of grains, ρ_g is the mass density of grains, and K is a proportionality constant. However, the origin of the scaling laws involved in the earlier empirical formulas has been recently explored from the perspective of the PTT.[43]

The velocity v_l of a local turbulent eddy that controls the onset phenomenon can be scaled with the velocity scale V_L of large-scale eddies as $v_l \sim V_L (l/L)^{-(1+\sigma)/2}$, where σ signifies the typical spectral exponent;[43] for instance, in the energy inertial range that follows the Kolmogorov scaling, $\sigma = -5/3$. When the l approaches the grain size d and having considered $V_L \sim U$, the fluid-particle interplay in the vicinity of the granular bed produces

$$\tau \sim \rho_f U v_d \sim \rho_f U^2 N^{-(1+\sigma)/2}. \tag{12}$$

At an onset of grain motion, it follows $\tau \sim \Delta \rho_f g d \Theta_c$, where Θ_c [$= u_{*c}^2/(\Delta g d)$] is the critical Shields number and u_{*c} is the critical shear velocity.[44] Therefore, Eq. (12) leads to

$$F_{dc} \sim N^{(1+\sigma)/4}, \tag{13}$$

which reflects that the F_{dc} obeys the "$(1 + \sigma)/4$" scaling law with N. Figure 5(a) sheds light on the dependency of F_{dc} on N covering a wide range of N.[43] In the energy inertial range, the application of $\sigma = -5/3$ yields $F_{dc} \sim N^{-1/6}$, corroborating the Manning-Strickler relationship. For $N < 10^{-4}$, the grain size closely approaches the viscous sublayer thickness, which acts as a barrier to shield the grains, prohibiting the outer flow to sense the bed roughness. It ensures a hydraulically smooth flow regime, which is governed by the viscous momentum transfer. Under this circumstance, the energy spectrum obeys

$\sigma = -3$ due to the existence of the enstrophy cascade[45] that results from the smooth velocity field to produce $F_{dc} \sim N^{-1/2}$. On the other hand, for $N \geq 10^{-1}$, the energy spectrum displays $\sigma = -1$ due to the presence of large-scale eddies belonging to the energy containing range and as a result $F_{dc} \sim N^0$. In addition, Figs. 5(b)–5(d) present the comparison of the scaling laws of $F_{dc}(N)$ in three separate windows of N with the primitive empirical formulas reported in the literature.[46–50] For different windows of N, the deviation of the empirical formulas from the spectral laws is attributed to the uncertainties involved in the experimental data.

B. Bedload transport

The sediment grains are set in motion when the bed shear stress τ_0 exceeds the critical bed shear stress τ_{0c} for the grain motion. The grains are transported within a thin layer, known as the *bedload layer*,[10] in different modes of transport, for instance, rolling mode (RM), sliding mode (SM), and lifting mode (LM) of transport, as sketched in Fig. 6. Previous experimental and analytical studies revealed that the nondimensional bedload flux Φ_b [$= q_b/(\Delta g d^3)^{1/2}$] follows $\Phi_b \sim T_*^{3/2}$,[10] where q_b is the amount of grain (solid) volume transported per unit time and width, T_* [$= (\tau_0 - \tau_{0c})/\tau_{0c} = (\Theta - \Theta_c)/\Theta_c$] is the transport stage parameter, and Θ [$= u_*^2/(\Delta g d)$] is the Shields number. It has been recently shown that the above scaling law can be deduced applying the simple phenomenological arguments.[43] If n is the number of grains per unit area of the granular bed and v_p is the grain velocity, then $q_b \sim n d^3 v_p$. Following the traditional arguments of bedload transport,[10,51] the bed shear stress τ_0 can be split into the dispersive particle shear stress τ_{0p} and the interfacial fluid shear stress τ_{0f}. This formulation accounts for the shear between the layers of grains and the shear between the grains and the surrounding fluid. When the bedload transport takes place, the τ_{0f} equals to the τ_{0c}, suggesting that the τ_{0c} acts directly on the immobile grains as a
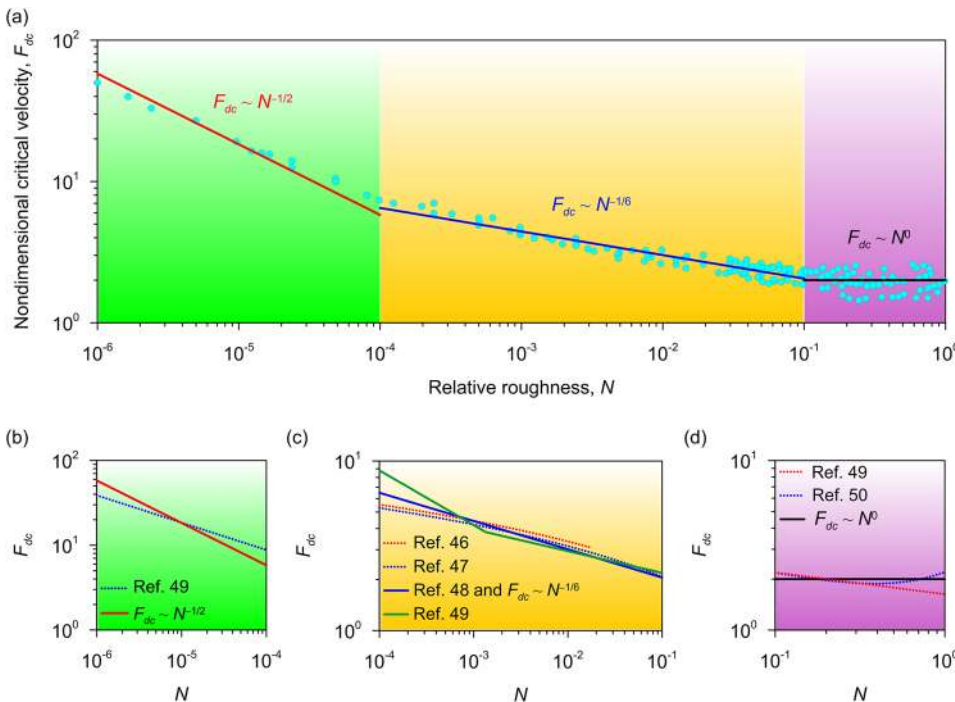
FIG. 5. (a) Spectral link between the nondimensional critical velocity F_{dc} and the relative roughness N in three different windows of N.[43] (b–d) Comparison of the scaling laws of $F_{dc}(N)$ obtained from the perspective of the PTT[43] with the primitive empirical formulas.[46–50]
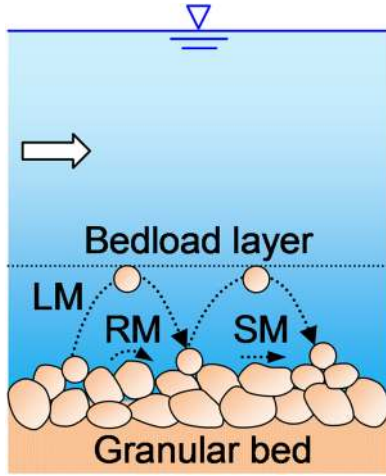
FIG. 6. Schematic illustration of grain transport as a bedload. The rolling mode (RM), sliding mode (SM), and lifting mode (LM) of grain transport are also shown.

skin frictional stress leaving the available stress $\tau_0 - \tau_{0c}$ to act on the mobile grains as a form drag induced stress. Thereafter, it was shown that $n \sim (\Theta - \Theta_c)/d^2$ and $v_p \sim U_c[(\Theta/\Theta_c) - 1]^{1/2}$ yielding

$$\Phi_b \sim T_*^{3/2} N^{(1+\sigma)/4}. \tag{14}$$

Equation (14) confirms the emergence of $\Phi_b \sim T_*^{3/2}$ scaling law in the earlier empirical formulas.[10]

C. Suspended load transport

Large channel carries huge quantity of suspended sediments along its course; for instance, recent US Geological Survey of suspended sediment samples collected from fourteen sites during 2007–2011 reported that the Minnesota River annually carried the mean suspended load of approximately 1.8×10^6 tons.[52] Channels carrying extreme suspended sediment load may cause serious damage for flood control, irrigation and navigation, soil conservation, and eutrophication causing nutrients, suggesting a necessity of proper estimation, and monitoring of suspended load transport. In the case of sediment suspension (Fig. 7), the sediment grains are carried
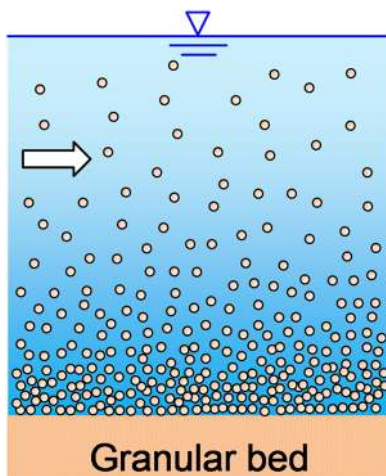
FIG. 7. Schematic illustration of grain transport as a suspended load.

by the neighboring fluid for a sufficiently long time. The turbulent eddies grip the suspended grains within their core making a convective transport of grains from a zone of higher to lower concentrations obeying the Fickian diffusion. The suspended load is usually determined from the integration of the product of the suspended sediment concentration and the time-averaged flow velocity distributions over the entire depth of the channel. Long ago, an analytical solution of the distribution of suspended sediment concentration in the vertical was obtained by solving the advection-diffusion equation of suspended sediment motion.[53] In solving the advection-diffusion equation, the classical law of the wall and the Fickian diffusion were used. In recent years, the distribution of suspended sediment concentration in the vertical was obtained by means of the power law theory[54] and the energetics of the two-phase flow.[55] However, within the turbulent wall-shear layer, the distribution of suspended sediment in the vertical obeys a power law as

$$\frac{C(z)}{C_R} = \left(\frac{z}{z_R}\right)^{-Z}, \tag{15}$$

where $C(z)$ is the sediment concentration at any level z normalized by the reference concentration C_R at a distance z_R from the channel bed and Z is the *Rouse number*. Recent application of the PTT has evidenced this power law behavior by providing a simple sediment flux balance model under equilibrium state.[43] The Rouse equation falls short in deriving this power law because of the questionable assumptions involved in the derivation.[10] The power law also provided a simple interpretation to find the Rouse number within the turbulent wall-shear layer for a given concentration distribution.

D. Formation of an erosion pit under equilibrium state

The formation of an erosion pit, which is also often called a *pothole* or a *giant's kettle*, caused by a waterfall or a swift turbulent flow is a natural phenomenon. The turbulent channel erodes large amounts of bed sediments and, sometimes, prolonged erosion can even create deep canyons; for example, the Grand Canyon carved by the Colorado River. The application of this phenomenon poses a relevant question: For a given power of the waterfall, what is the depth of the erosion pit under equilibrium state? By contrast, the inverse problem is to ascertain the flow discharge that engraved the terrestrial channel bed to form giant depression. In fluvial hydraulics, this phenomenon is quite common downstream of a drop structure and it may imperil the stability of the structure. Here, we highlight the scaling law involved in such a phenomenon under three different circumstances, such as the formation of an erosion pit due to a fluid jet (Fig. 8), around a cylinder (Fig. 9), and in a channel contraction (Fig. 10).

When a fluid jet impinges on a water body, a turbulent cauldron is formed. Due to the jet energetics, the turbulent cauldron erodes the granular bed to form an erosion pit (Fig. 8). The depth of the erosion pit increases until an equilibrium state is attained between the turbulent cauldron and the granular bed. For a given power P of the jet per unit thickness, the jet discharge q per unit thickness, the jet head h_0, and the grain size d, the researchers paid a considerable heed to find the
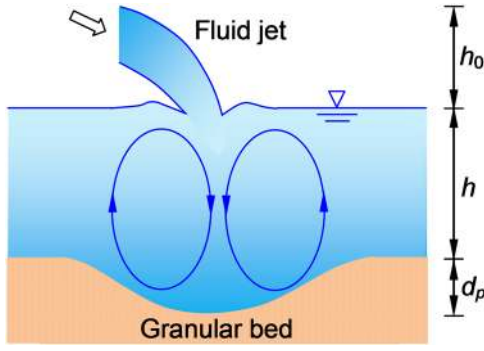
FIG. 8. Schematic illustration of an erosion pit with a turbulent cauldron triggered by a fluid jet. The fluid jet, from a height h_0 called the *jet head*, plunges into the water body having a depth h and creates an erosion pit of depth d_p.
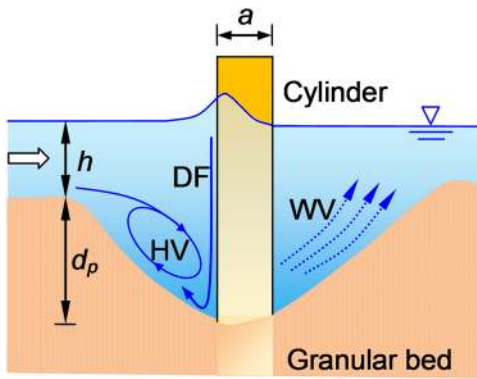
FIG. 9. Schematic illustration of an erosion pit of depth d_p formed around a circular cylinder of diameter a embedded in a granular bed. Here, h is the flow depth upstream of the erosion pit, HV is the horseshoe vortex, DF is the downflow, and WV is the wake vortices.

equilibrium depth of the erosion pit. If D is the sum of the depth of the erosion pit and the water body ($D = d_p + h$), a general scaling law can be written as

$$D \sim \frac{q^{\alpha_q} h_0^{\alpha_{h_0}} g^{\alpha_g} d^{\alpha_d}}{\Delta^{\alpha_\Delta}}, \qquad (16)$$

where the exponents α_q, α_{h_0}, α_g, α_d, and α_Δ predicted by the different empirical formulas vary significantly.[10] Applying the dimensional analysis and the similarity methods, it can be found that $P = \rho_f g^{3/2} D^{5/2} f(d/D, \rho_g/\rho_f)$. In the case of an incomplete similarity, $P = \rho_f g^{3/2} D^{5/2} (d/D)^{\alpha} f[\rho_g/\rho_f + O(d/D)^{\alpha}]$, where α is the similarity exponent, and after some algebra, the D takes the form

$$D \sim q^{\alpha_q} h_0^{\alpha_{h_0}} g^{\alpha_g} d^{\alpha_d} f_1 \left(\frac{\rho_g}{\rho_f} \right), \qquad (17)$$

where $\alpha_q = \alpha_{h_0} = 2/(5 - 2\alpha)$, $\alpha_g = -1/(5 - 2\alpha)$, $\alpha_d = -2\alpha/(5 - 2\alpha)$, and $f_1 \sim 1/f^{2/(5-2\alpha)}$. This form of D is linked with the salient variables of the problem via a single parameter α, which was obtained from the perspective of the PTT.[56,57] The jet power per unit jet thickness is $P = gq\rho_f h_0$. The P can also be thought as a product of the local dissipation rate ε ($\sim V_L^3/D$) and the fluid mass M per unit thickness of the turbulent cauldron ($M \sim \rho_f D^2$). This makes $V_L \sim (gqh_0/D)^{1/3}$. The Reynolds shear stress τ at the surface of the erosion pit follows $\tau \sim \rho_f V_L v_l$, where the velocity scale of the turbulent eddies v_l can be scaled as $v_l \sim V_L(l/L)^{1/3}$. In the limit $l \sim d$ and $L \sim D$, it follows

$$\tau \sim \frac{\rho_f (gqh_0)^{2/3} d^{1/3}}{D}. \qquad (18)$$

As the erosion pit deepens with time, the size of the turbulent cauldron becomes larger and in turn, the strength of the turbulent cauldron weakens according to the scaling $V_L \sim (gqh_0/D)^{1/3}$, making a reduction in the shear stress exerted on the granular bed surface. In due course, the depth of the erosion pit attains an equilibrium state, where the bed shear stress equals the critical bed shear stress for the motion of sediment grains. For a constant value of critical Shields number Θ_c, the scaling $\tau \sim \tau_{0c} \sim \Delta \rho_f g d$ makes

$$D \sim \frac{q^{2/3} h_0^{2/3} g^{-1/3} d^{-2/3}}{\Delta}, \qquad (19)$$

which indicates $\alpha_q = \alpha_{h_0} = 2/3$, $\alpha_g = -1/3$, $\alpha_d = -2/3$, and $\alpha = 1$.

The formation of an erosion pit around a cylinder embedded in a granular bed remains a challenging problem of fluvial hydraulics in the context of the stability of bridge pier foundation (Fig. 9). The presence of the cylinder causes a 3D flow separation giving rise to a vortex flow around and a vortex shedding downstream of the cylinder. The approach flow gets separated at the upstream face of the cylinder causing to form the horseshoe vortex (HV) as depicted in Fig. 9. It subsequently traverses the downstream to create an erosion pit due to the removal of sediment grains. In addition, at the upstream face of the cylinder, a reduction of the stagnation pressure in the downward direction creates a downflow (DF), which dislodges the grains, and consequently, the grains are transported by the action of the HV along the upstream slope of the erosion pit (Fig. 9). Downstream of the cylinder, the wake vortices (WV), behaving like a tornado, lifts off the sediment grains by the action of vortex suction.[10] In an attempt to seek the scaling law of the depth of the erosion pit from the viewpoint of the PTT, the length scale of the large-scale eddy was surmised as to scale with the equilibrium depth of the erosion pit, $L \sim d_p$.[58] The power P accompanying the large-scale eddy was determined as the work done by the drag force f_D acting on

FIG. 10. Schematic illustration of an erosion pit of depth d_p formed in a channel contraction. In plan view (*left*), B_1 and B_2 are the channel widths corresponding to the approach and contracted channel sections, respectively, whereas in elevation view (*right*), h_1 and h_2 are the flow depths in those sections.
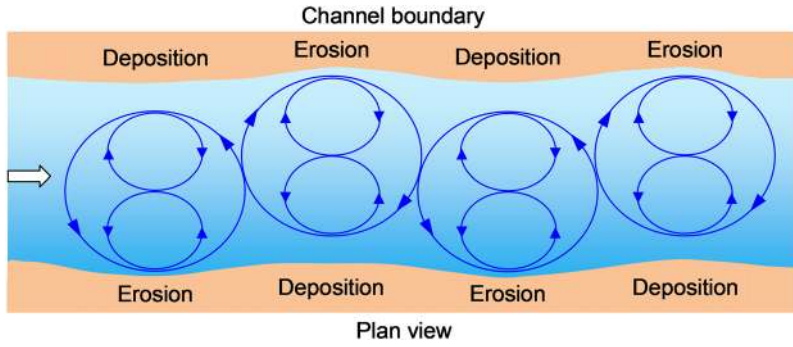
FIG. 11. Schematic illustration of the onset of meandering of a straight channel displaying the counter-rotation of contiguous large-scale eddies in succession to cause the processes of alternate erosion and deposition of grains (plan view).

the cylinder ($P = f_D U$). The f_D per unit length of the cylinder can be expressed as $f_D = (1/2)\rho_f C_D a U^2$, where C_D is the drag coefficient and a is the cylinder diameter. The mass of the largest eddy per unit length L follows $M \sim \rho_f L^2$, resulting in $\varepsilon = P/M \sim C_D a U^3/L^2$, which was equated to $\varepsilon \sim V_L^3/L$ to produce $V_L \sim U(aC_D/L)^{1/3} \sim U(aC_D/d_p)^{1/3}$. The Reynolds shear stress τ was obtained as

$$\tau \sim \rho_f V_L^2 \left(\frac{d}{d_p}\right)^{1/3} \sim \rho_f U^2 \left(\frac{aC_D}{d_p}\right)^{2/3}\left(\frac{d}{d_p}\right)^{1/3}. \quad (20)$$

Under equilibrium state ($\tau \sim \tau_{0c} \sim \Delta\rho_f gd$), the scaling law of d_p was thus anticipated as[58]

$$\frac{d_p g}{U^2} \sim \left(\frac{a}{d}\right)^{2/3}\frac{C_D^{2/3}}{\Delta}. \quad (21)$$

In practice, wide channels are often contracted to construct various kinds of hydraulic structures, such as bridges, weirs, guide banks, and many others. The formation of an erosion pit in a channel contraction is another important aspect (Fig. 10). When an approach channel flow, having a channel width B_1 and flow depth h_1, enters into a contracted channel through a gradual transition, having a contracted channel width B_2 and flow depth h_2, the flow in the contracted zone is accelerated. It leads to a higher flow velocity giving rise to a larger bed shear stress that erodes the granular bed forming an erosion pit in the contracted portion of the channel. Let D be the sum of the equilibrium depth of the erosion pit and the approach flow depth ($D = d_p + h_1$). To seek an appropriate scaling law of D, using the dimensional analysis, it was linked with the nondimensional approach flow velocity F_{d1} [$= U_1/(\Delta gd)^{1/2}$], the approach relative roughness N_1 ($= d/h_1$), and the channel contraction ratio r ($= B_2/B_1$).[43] Applying the continuity equation ($U_1 h_1 B_1 = U_2|_{U_2=U_c} h_2 B_2$) and overlooking the difference in velocity heads and the energy loss through the channel transition ($d_p = h_2 - h_1$) produce $D/h_1 = U_1/(r\, U_2|_{U_2=U_c})$. In the energy inertial range, using the scaling law of the critical velocity in the contracted channel as $U_2|_{U_2=U_c} \sim (\Delta gd)^{1/2}(D/h_1)^{1/6}N_1^{-1/6}$, the scaling law of D was predicted as[43]

$$\frac{D}{h_1} \sim F_{d1}^{6/7} r^{-6/7} N_1^{1/7}. \quad (22)$$

E. Onset of meandering of a straight channel

Meandering channels are ubiquitous features of planetary surfaces. A central aspect is the onset of meandering of a

channel. To find its underlying mechanism, the motion of the turbulent eddies in a straight channel was considered analogous to that of contiguous solid spherical balls, arranged in a row, confined to two parallel boundaries.[59] As soon as the first sphere is given a counter rotational motion having a trivial shift toward the right-side boundary, the next neighboring sphere displays a clockwise rotation having a similar shift toward the left-side boundary. For the remaining spheres in succession, similar kinds of processes of alternate rotation and shift take place, as if a meandering path is formed by the line connecting the centers of the spheres. In close proximity of the granular bed, the anisotropic turbulence stretches the turbulent eddies, forming the turbulence induced secondary currents.[10] When a highly intermittent counter rotating large-scale eddy erodes the grains close to the right-side channel boundary (Fig. 11), the eroded grains are deposited at the opposite side of the channel boundary. The subsequent adjacent local eddy is motivated by the motion of the parent eddy, and thus, it performs a clockwise rotation having shifted toward the left-side channel boundary. In this manner, the processes of alternative erosion and deposition advance. Then, a quantitative criterion of this phenomenon was obtained by applying the equal periodicity concept.[60] With this concept and using the spectral link of the mean flow velocity,[11] a unique scaling law was deduced connecting the streamwise bed slope S_0, channel width B, flow discharge Q, and grain size d. The streamwise bed slope corresponding to the onset of meandering was anticipated as[59]

$$S_0 \sim B^{2/9} Q^{-2/9} d^{1/3} g^{1/9}, \quad (23)$$

which agrees satisfactorily with myriads of experimental data collected from laboratory and field.[59]

IV. CONCLUSION

The impact of the phenomenological theory of turbulence (PTT), highlighting its recent advances over the past two decades to answer apparently unrelated and unresolved issues, on the pragmatic approach to fluvial hydraulics has been elucidated. This theory delivers a smart strategy to find the fingerprint of turbulence in the form of scaling laws that are involved in several fluid flow phenomena, and thus, it has the foresight to verify the accuracy of various empirical formulas pertaining to fluvial hydraulics. It suffices here to say that the application of the PTT has explained the physical processes with much simplicity and intuition, as if to remind us of the

words of Richard Feynman: "The true hallmark of genius is the ability to explain things simply." The application of this theory makes it possible to bring theory and practice under one umbrella, explaining the origin of the empirical formulas and dictating the uncertainty that lingers in the experimental observations. The PTT permits us to find the scaling laws of many other key physical processes, where the turbulence is inextricably linked with, for instance, the scaling law of mean evaporation rate from rough surfaces into the turbulent atmosphere.[61]

One of the cornerstones of the PTT is the existence of the universal energy spectrum–eddy wavenumber dependency (Kolmogorov spectrum) in the energy inertial range. However, in natural gravel or boulder streambeds, this universality can slightly break down from the idealized notion depending on the bed roughness heterogeneity and the levels of turbulence anisotropy.[62] A new phenomenological model can be built to address such complexities by which more insights into the flow physics can be gleaned. In essence, an enriched understanding of the subject can help us to seek the scaling and similarity laws of several complex processes guided by the turbulence and their possible origin as a future scope of research.

[1] J. I. Cardesa, A. Vela-Martín, and J. Jiménez, "The turbulent cascade in five dimensions," Science **357**, 782–784 (2017).

[2] A. N. Kolmogorov, "The local structure of turbulence in incompressible viscous fluids at very large Reynolds numbers," Dokl. Akad. Nauk SSSR **30**, 299–303 (1941).

[3] U. Frisch, *Turbulence: The Legacy of A. N. Kolmogorov* (Cambridge University Press, Cambridge, 1995).

[4] K. R. Sreenivasan and R. A. Antonia, "The phenomenology of small-scale turbulence," Annu. Rev. Fluid Mech. **29**, 435–472 (1997).

[5] T. Ishihara, T. Gotoh, and Y. Kaneda, "Study of high-Reynolds number isotropic turbulence by direct numerical simulation," Annu. Rev. Fluid Mech. **41**, 165–180 (2009).

[6] D. P. Ruelle, "Hydrodynamic turbulence as a problem in nonequilibrium statistical mechanics," Proc. Natl. Acad. Sci. U. S. A. **109**, 20344–20346 (2012).

[7] J. Schumacher, J. D. Scheel, D. Krasnov, D. A. Donzis, V. Yakhot, and K. R. Sreenivasan, "Small-scale universality in fluid turbulence," Proc. Natl. Acad. Sci. U. S. A. **111**, 10961–10965 (2014).

[8] J. C. Vassilicos, "Dissipation in turbulent flows," Annu. Rev. Fluid Mech. **47**, 95–114 (2015).

[9] I. Marusic, R. Mathis, and N. Hutchins, "Predictive model for wall-bounded turbulent flow," Science **329**, 193–196 (2010).

[10] S. Dey, *Fluvial Hydrodynamics: Hydrodynamic and Sediment Transport Phenomena* (Springer-Verlag, Berlin, Germany, 2014).

[11] G. Gioia and F. A. Bombardelli, "Scaling and similarity in rough channel flows," Phys. Rev. Lett. **88**, 014501 (2002).

[12] G. Gioia and P. Chakraborty, "Turbulent friction in rough pipes and the energy spectrum of the phenomenological theory," Phys. Rev. Lett. **96**, 044502 (2006).

[13] G. G. Katul, A. Porporato, C. Manes, and C. Meneveau, "Co-spectrum and mean velocity in turbulent boundary layers," Phys. Fluids **25**, 091702 (2013).

[14] B. Cipra, "A new theory of turbulence causes a stir among experts," Science **272**, 951 (1996).

[15] R. L. Panton, "Review of wall turbulence as described by composite expansions," Appl. Mech. Rev. **58**, 1–36 (2005).

[16] G. I. Barenblatt and A. Chorin, "New perspectives in turbulence: Scaling laws, asymptotics, and intermittency," SIAM Rev. **40**, 265–291 (1998).

[17] G. I. Barenblatt and A. Chorin, "A mathematical model for the scaling of turbulence," Proc. Natl. Acad. Sci. U. S. A. **101**, 15023–15026 (2004).

[18] G. Gioia and P. Chakraborty, "Spectral derivation of the classic laws of wall-bounded turbulent flows," Proc. R. Soc. A **473**, 20170354 (2017).

[19] G. Gioia, N. Guttenberg, N. Goldenfeld, and P. Chakraborty, "Spectral theory of the turbulent mean-velocity profile," Phys. Rev. Lett. **105**, 184501 (2010).

[20] G. G. Katul and C. Manes, "Cospectral budget of turbulence explains the bulk properties of smooth pipe flow," Phys. Rev. E **90**, 063008 (2014).

[21] S. B. Pope, *Turbulent Flows* (Cambridge University Press, Cambridge, 2000).

[22] A. A. R. Townsend, *The Structure of Turbulent Shear Flow* (Cambridge University Press, Cambridge, 1976).

[23] J. L. Lumley, "Similarity and the turbulent energy spectrum," Phys. Fluids **10**, 855–858 (1967).

[24] S. G. Saddoughi and S. V. Veeravalli, "Local isotropy in turbulent boundary layers at high Reynolds number," J. Fluid Mech. **268**, 333–372 (1994).

[25] R. W. Powell, "History of Manning's formula," J. Geophys. Res. **65**, 1310–1311, https://doi.org/10.1029/jz065i004p01310 (1960).

[26] L. Wilson, G. J. Ghatan, J. W. Head III, and K. L. Mitchell, "Mars outflow channels: A reappraisal of the estimation of water flow velocities from water depths, regional slopes, and channel floor properties," J. Geophys. Res. **109**, E09003, https://doi.org/10.1029/2004je002281 (2004).

[27] G. Gioia, P. Chakraborty, and F. A. Bombardelli, "Rough-pipe flows and the existence of fully developed turbulence," Phys. Fluids **18**, 038107 (2006).

[28] S. Bonetti, G. Manoli, C. Manes, A. Porporato, and G. G. Katul, "Manning's formula and Strickler's scaling explained by a co-spectral budget model," J. Fluid Mech. **812**, 1189–1212 (2017).

[29] C. Manes, L. Ridolfi, and G. Katul, "A phenomenological model to describe turbulent friction in permeable-wall flows," Geophys. Res. Lett. **39**, L14403, https://doi.org/10.1029/2012gl052369 (2012).

[30] S. Wang, Y. Zhou, M. M. Alam, and H. Yang, "Turbulent intensity and Reynolds number effects on an airfoil at low Reynolds numbers," Phys. Fluids **26**, 115107 (2014).

[31] M. Mafi, "Investigation of turbulence created by formula One™ cars with the aid of numerical fluid dynamics and optimization of overtaking potential," in *ANSYS Conference and 25th CADFEM Users' Meeting* (Congress Center Dresden, Germany, 2007), pp. 1–10.

[32] Y. Ito, T. Watanabe, K. Nagata, and Y. Sakai, "Turbulent mixing of a passive scalar in grid turbulence," Phys. Scr. **91**, 074002 (2016).

[33] T. Banerjee and G. G. Katul, "Logarithmic scaling in the longitudinal velocity variance explained by a spectral budget," Phys. Fluids **25**, 125106 (2013).

[34] G. G. Katul, T. Banerjee, D. Cava, M. Germano, and A. Porporato, "Generalized logarithmic scaling for high-order moments of the longitudinal velocity component explained by the random sweeping decorrelation hypothesis," Phys. Fluids **28**, 095104 (2016).

[35] R. A. Antonia and M. R. Raupach, "Spectral scaling in a high Reynolds number laboratory boundary layer," Boundary Layer Meteorol. **65**, 289–306 (1993).

[36] V. Nikora, "Origin of the "−1" spectral law in wall-bounded turbulence," Phys. Rev. Lett. **83**, 734–736 (1999).

[37] I. Marusic, J. P. Monty, M. Hultmark, and A. J. Smits, "On the logarithmic region in wall turbulence," J. Fluid Mech. **716**, R3 (2013).

[38] M. Calaf, M. Hultmark, H. J. Oldroyd, V. Simeonov, and M. B. Parlange, "Coherent structures and the k^{-1} spectral behavior," Phys. Fluids **25**, 125107 (2013).

[39] M. Wilczek, R. J. A. M. Stevens, and C. Meneveau, "Spatio-temporal spectra in the logarithmic layer of wall turbulence: Large-eddy simulations and simple models," J. Fluid Mech. **769**, R1 (2015).

[40] M. H. Carr, "The fluvial history of Mars," Philos. Trans. R. Soc., A **370**, 2193–2215 (2012).

[41] V. R. Baker, C. W. Hamilton, D. M. Burr, V. C. Gulick, G. Komatsu, W. Luo, J. W. Rice, Jr., and J. A. P. Rodriguez, "Fluvial geomorphology on Earth-like planetary surfaces: A review," Geomorphology **245**, 149–182 (2015).

[42] A. Mathur and D. da Cunha, *Mississippi Floods: Designing a Shifting Landscape* (Yale University Press, 2001).

[43] S. Z. Ali and S. Dey, "Origin of the scaling laws of sediment transport," Proc. R. Soc. A **473**, 20160785 (2017).

[44] S. Z. Ali and S. Dey, "Hydrodynamics of sediment threshold," Phys. Fluids **28**, 075103 (2016).

[45] R. H. Kraichnan, "Inertial ranges in two-dimensional turbulence," Phys. Fluids **10**, 1417–1423 (1967).

[46] E. E. Lavy, *River Mechanics* (National Energy Press, Moscow, 1956).

[47] V. N. Goncharov, *Dynamics of Channel Flow* (Israel Programme for Scientific Translation, Moscow, 1964).

[48]C. R. Neill, "Note on initial movement of coarse uniform bed-material," J. Hydraul. Res. **6**, 173–176 (1968).

[49]M. García-Flores and J. A. Maza-Alvarez, *Inicio de Movimiento y Acorazamiento*, Series del Instituto de Ingeniería Vol. 592 (Capítulo 8 del Manual de Ingeniería de Ríos, UNAM, Mexico, 1997).

[50]J. Aguirre-Pe, M. L. Olivero, and A. T. Moncada, "Particle densimetric Froude number for estimating sediment transport," J. Hydraul. Eng. **129**, 428–437 (2003).

[51]R. A. Bagnold, "The flow of cohesionless grains in fluids," Proc. R. Soc. A **249**, 235–297 (1956).

[52]C. A. Ellison, B. E. Savage, and G. D. Johnson, Suspended-Sediment Concentrations, Loads, Total Suspended Solids, Turbidity, and Particle-Size Fractions for Selected Rivers in Minnesota, Scientific Investigations Report 2013–5205, U.S. Geological Survey, USA, 2007–2011.

[53]H. Rouse, "Modern conceptions of the mechanics of turbulence," Trans. Am. Soc. Civ. Eng. **102**, 463–505 (1937).

[54]F. N. Cantero-Chinchilla, O. Castro-Orgaz, and S. Dey, "Distribution of suspended sediment concentration in wide sediment-laden streams: A novel power-law theory," Sedimentology **63**, 1620–1633 (2016).

[55]S. Z. Ali and S. Dey, "Mechanics of advection of suspended particles in turbulent flow," Proc. R. Soc. A **472**, 20160749 (2016).

[56]G. Gioia and F. A. Bombardelli, "Localized turbulent flows on scouring granular beds," Phys. Rev. Lett. **95**, 014501 (2005).

[57]F. A. Bombardelli and G. Gioia, "Scouring of granular beds by jet-driven axisymmetric turbulent cauldrons," Phys. Fluids **18**, 088101 (2006).

[58]C. Manes and M. Brocchini, "Local scour around structures and the phenomenology of turbulence," J. Fluid Mech. **779**, 309–324 (2015).

[59]S. Dey and S. Z. Ali, "Origin of the onset of meandering of a straight river," Proc. R. Soc. A **473**, 20170376 (2017).

[60]P. W. Werner, "On the origin of river meanders," Trans., Am. Geophys. Union **32**, 898–902 (1951).

[61]G. Katul and H. Liu, "A Kolmogorov-Brutsaert structure function model for evaporation into a turbulent atmosphere," Water Resour. Res. **53**, 3635–3644, https://doi.org/10.1002/2016wr020006 (2017).

[62]D. Ferraro, S. Servidio, V. Carbone, S. Dey, and R. Gaudio, "Turbulence laws in natural bed flows," J. Fluid Mech. **798**, 540–571 (2016).